An Auto Disturbance Rejection Control Method for Four Rotor UAV Flight Operation

Dai Wan[1](✉), Simin Peng[1], Jinliang Li[1], Liang Peng[2], Yingying Yi[3], and Zoujun Wang[1]

[1] State Grid Hunan Electric Power Company Limited Research Institute, Changsha 410007, China
280241509@qq.com
[2] Changsha University of Science and Technology, Changsha 410000, China
[3] Changsha Tax Service, Changsha 410000, China

Abstract. The four rotor unmanned aerial vehicle (UAV) can carry out all-round and efficient inspection of power equipment. At present, the four rotor UAV has become an essential equipment in the inspection of transmission lines. However, the support of UAV for distribution line inspection is far less than that for transmission line inspection. This is mainly because the operating environment of distribution lines is much more complex and harsh than that of transmission lines. In the process of power distribution line inspection, all kinds of environmental interference are far more than transmission lines. The existing four rotor UAV control methods have poor resistance to external interference. Aiming at the above problems, the research on ADRC method of four rotor UAV is carried out in this paper. The principle of active disturbance rejection is analyzed. A linear active disturbance rejection scheme is proposed. The attitude control module of UAV is designed. The simulation model of ADRC system of four rotor UAV is constructed. The simulation results show that the ADRC method can effectively alleviate the influence of random interference on the flight state of UAV. For the UAV operating in complex environment, it is necessary to optimize the anti-interference of its control system. The research results have guiding significance for improving the anti-interference ability of UAV in the process of distribution line inspection.

Keywords: Four Rotor Unmanned Aerial Vehicle · Auto Disturbance Rejection Control · Control Method

1 Introduction

With the continuous improvement of national living standards, people have higher and higher requirements for the reliability of power supply. However, in recent years, the scale of distribution lines and equipment has become larger and larger. The traditional manual inspection mode has been unable to cope with the large-scale inspection objects and the requirements of lean inspection work. The emergence of unmanned aerial vehicle inspection technology provides new technical means for power grid operation and

H. Yang et al. (Eds.): SmartGIFT 2022, LNICST 483, pp. 466–477, 2023.
https://doi.org/10.1007/978-3-031-31733-0_40

maintenance personnel [1]. At present, unmanned aerial vehicle inspection technology has been widely used in the field of power grid, and has achieved good application results. Especially in the field of power transmission, UAV Patrol has become a very mature operation mode [2]. However, UAV inspection technology is still in its infancy in the field of power distribution. Because the operating environment of distribution lines is far more complex and harsh than that of transmission lines, UAV will face a lot of environmental interference during patrol inspection. The existing flight state control system of four rotor UAV is difficult to adapt to the complex operating environment of distribution network [3].

At present, most of the multi rotor UAV use proportional integral derivative (PID) control system. PID control technology is a relatively mature technology. The PID control system can adjust the output response of the system according to the error signal of the feedback loop, so as to reduce the error with the expected input [4]. In the current mainstream engineering control, PID is still a very excellent solution. However, the performance of PID control method is not satisfactory in the face of complex systems. In the face of multiple disturbances, the control effect of PID is seriously affected by the disturbance [5]. With the continuous development of control technology, there are many modern control technology theories that pursue high-precision control effect. However, these modern control theories, which strongly rely on accurate models, are difficult to realize in practical engineering applications. In view of the above problems, academia has proposed an active disturbance rejection control (ADRC) method. Active disturbance rejection control method is evolved from PID control method. Suppose that there is a total disturbance consisting of internal disturbance and external disturbance in the control system. After assuming this uncertain fuzzy model, extended state observer (ESO) is used for observation. The result of ESO observation can be regarded as the total disturbance of the system. Therefore, we can build this system into a series integral system through ESO. Then create an nonlinear state error feedback control law (NSEF) to realize the interference suppression of the total disturbance of the system, which can make the system obtain better control effect and system stability [4].

This paper deeply analyzes the principle of ADRC. Tracking differential controller (TD), extended state observer (ESO) and nonlinear state error feedback control law (NSEF) are designed. A linear active disturbance rejection control method is proposed. The active disturbance rejection control model of four rotor UAV is constructed. The simulation test is carried out. The research results have guiding significance for improving the anti-interference ability and environmental adaptability of UAV.

2 Analysis of Active Disturbance Rejection Algorithm

2.1 Active Disturbance Rejection Principle

The core of active disturbance rejection control method is to regard the controlled object as a standard system with integral series connection. The ESO is used to estimate it. The estimation results are used to dynamically compensate the total disturbance of the system. ADRC is generally composed of three parts.

(1) Tracking differentiator
TD can track signals with random noise or discrete discontinuous signals. Its function is to improve the control quality of the system and simplify the structure of the control system. The TD can output two signals. They are the tracking signal and its differential signal. Among them, the tracking signal can be output through the fastest control synthesis function. Based on the above two signals, a transition process can be set in the closed-loop system. This transition process can not only reduce the overshoot of the control system, but also quickly respond to the control requirements of the system.
(2) Extended state observer
The ESO is the decision-making and observation mechanism of the control system. The ESO can not only observe the state of the controlled object, but also compensate the disturbance in the control system. The ESO does not need an accurate model when observing the state of the controlled object.
(3) Nonlinear state error feedback control law
The NSEF is similar to the control rule of PID. By calculating the tracking signal and differential signal output by the TD, corresponding groups of error signals can be generated. NSEF can be formed by nonlinear combination of error signals.

2.2 Analysis of Nonlinear Active Disturbance Rejection Algorithm

In the nonlinear ADRC method, the ESO is designed by using fal function. The control system is designed by using the nonlinear combination of fal function and the fastest control synthesis function fhan. The control system needs to meet two rules. First, large gain corresponds to small system error state. Second, small gain corresponds to large system error state. This design scheme can effectively eliminate the disturbance in the uncertain model. The problem of overshooting and system response speed can be solved simultaneously with only a set of parameters. The structure of the nonlinear ADRC system is shown in Fig. 1.

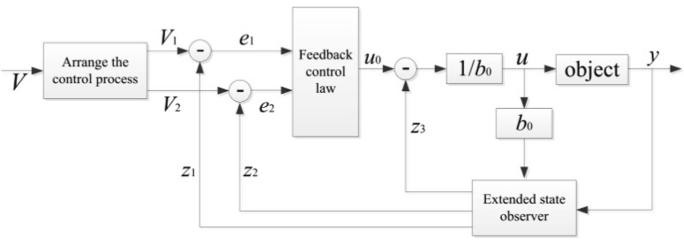

Fig. 1. Structure diagram of nonlinear ADRC system

First, the TD is designed. Suppose a second-order uncertain controlled object is $x^{(n)}$.

$$x^{(n)} = f(x, \dot{x}, \cdots, x^{(n-1)}, t) + w(t) + b(t)u(t) \tag{1}$$

where, $f(x, \dot{x}, \cdots, x^{(n-1)}, t)$ and $b(t)$ represent unknown functions. $u(t)$ represents the input control quantity. $w(t)$ represents the unknown disturbance function.

In order to make the system input smooth and not affected by sudden change interference, a transition process is designed in the system control flow. This transition process can make the system track the input signal quickly and reduce sudden change interference. Suppose the input signal of the TD is $u(t)$. It will output two signals, $x_1(t)$ and $x_2(t)$. $x_1(t)$ is the tracking signal of $u(t)$. $x_2(t)$ is the differential signal of the tracking signal $x_1(t)$. Similarly, $x_1(t)$ can be regarded as the differential signal of the input signal $u(t)$.

The expression of the second-order system is as follows.

$$\begin{cases} x_1(k+1) = x_1(k) + h \times x_2(k) \\ x_2(k+1) = x_2(k) + h \times u \, |u| \leqslant r \end{cases} \tag{2}$$

The second-order discrete system expression of the TD is as follows.

$$\begin{cases} x_1(k+1) = x_1(k) + h \times x_2(k) \\ x_2(k+1) = x_2(k) + h \times fst(x_1(k) - v(k), x_2(k), r, h) \, |u| \leqslant r \end{cases} \tag{3}$$

where $fst(\bullet)$ is the fastest control synthesis function. $fst(\bullet)$ is defined as follows.

$$\begin{aligned} & d = rd \\ & d_0 = hd \\ & y = (x_1(k) - v(k) + hx_2(k)) \\ & a_0 = \sqrt{d^2 + 8r|y|} \\ & a = \begin{bmatrix} x_2(k) + \frac{(a_0-d)}{2} \operatorname{sgn} \ y & |y| < d_0 \\ x_2(k) + \frac{y}{h} & |y| \leqslant d_0 \end{bmatrix} \\ & fhan = -\begin{bmatrix} r \ \operatorname{sgn} \ a & |a| > d \\ r\frac{a}{d} & |a| \leqslant d \end{bmatrix} \end{aligned} \tag{4}$$

where, h is the integration step factor. r is the tracking speed factor. R determines the speed of the tracking system. The larger r is, the faster the tracking input $u(t)$ of $x_1(t)$ is. h is the filter factor. h can eliminate the strong noise pollution in the input signal. However, if the value of h is too large, the tracking signal will be distorted and the tracking effect will become worse. Appropriate values of h and r should be selected.

Next, an ESO is designed. ESO is the most important module in NADRC system. The ESO is mainly responsible for real-time estimation of the current state of the control system and compensation of the disturbance of the control system. The disturbance estimated by ESO is called the expansion state of the total disturbance of the system. The expression of third-order ESO is as follows.

$$\begin{cases} \varepsilon_1 = z_1 - x_1 \\ \dot{z}_1 = z_2 - \beta_1 \varepsilon_1 \\ \dot{z}_2 = z_3 - \beta_2 fal(\varepsilon_1, \alpha_1, \delta) + bu \\ \dot{z}_3 = -\beta_3 fal(\varepsilon_1, \alpha_1, \delta) \end{cases} \tag{5}$$

where, β_1, β_2, β_3 and α_1 is greater than 0. α_2 is less than 1. The function expression of $fal(\bullet)$ is as follows.

$$fal(\varepsilon, \alpha, \delta) = \begin{cases} |\varepsilon|^{\alpha} sign(\varepsilon), |\varepsilon| > \delta \\ \varepsilon/\delta^{1-\alpha}, |\varepsilon| \leqslant \delta \end{cases} \quad (6)$$

Changing each variable in expression (7) can better observe the control system, so as to estimate the expanded state variables in real time.

Finally, the ESF is designed.

Finally, the NSEF is designed. NSEF can output a virtual control quantity u_0. u_0 can be used to control approximate integral series system. NSEF takes many forms. In general, the expression composed of U0 and disturbance estimator is as follows.

$$u = u_0 - z_3/b \quad (7)$$

where, b is the control gain of the uncertain object. b is an adjustable parameter.

2.3 Design of Linear Active Disturbance Rejection Control Method

The nonlinear auto disturbance rejection control (NADRC) system is simplified. Omit the TD module in the original scheme. The extended state observer and error feedback control law in the original scheme are optimized. A linear active disturbance rejection control (LADRC) system can be formed. The basic structure of linear auto disturbance rejection control system is shown in Fig. 2.

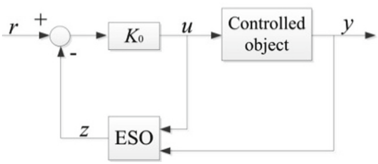

Fig. 2. Structure diagram of linear active disturbance rejection control system

When the control system meets any of the following three conditions, the linear extended state observer can be used. The first condition is that the system running time $t < T$. The second condition is that the tracking error of ESO is greater than 1. That is, $|e| > 1$. The third condition is that the total disturbance value of the system is greater than M. That is, $|z_{n+1}(k)| > M$. Where, M is an adjustable parameter. Assume that the general controlled object model is as follows.

$$\ddot{y} = bu(t) + f(x(t), u(t), d(t)) \quad (8)$$

where, f($x(t)$,$u(t)$,$d(t)$) is the total disturbance. B is the gain of the control channel. Therefore, the state space equation of the system is expressed as follows.

$$\begin{cases} \dot{x}_1 = x_2 \\ \dot{x}_2 = x_3 + bu \\ \dot{x}_3 = h \\ y = x_1 \end{cases} \quad (9)$$

Assume $z_1 = x_1, z_2 = \dot{x}_1 \cdot \cdot\cdot, z_n = x_1^{(n+1)}, z_{n+1} = f . f$ is a differentiable function. The following expression can be obtained by further calculation.

$$\begin{cases} \dot{z} = A_e z + B_e u + \dot{f} E_\mathrm{e} \\ x_1 = C_e u \end{cases} \tag{10}$$

where, the expression of each parameter is as follows.

$$z = \begin{bmatrix} z_1 \ z_2 \ z_3 \end{bmatrix}^T A_e = \begin{bmatrix} 0\,1\,0 \\ 0\,0\,1 \\ 0\,0\,0 \end{bmatrix}, B_e = \begin{bmatrix} 0 \\ b \\ 0 \end{bmatrix}, E_e = \begin{bmatrix} 0 \\ 0 \\ 1 \end{bmatrix}, C_e = \begin{bmatrix} 1\,0\,0 \end{bmatrix} \tag{11}$$

The expression of LADRC can be obtained as follows.

$$\begin{cases} \dot{z} = A_e z + B_e u + L(y - \dot{y}) \\ y = C_e z \end{cases} \tag{12}$$

$$L = \begin{bmatrix} \beta_1 \ \beta_2 \ \beta_3 \end{bmatrix}^T \tag{13}$$

where, L is the gain of the observer.

Take the derivatives of each order of the given input signal as v_i ($i = 1,2,\ldots, n$).

$$u = \frac{-z_3 + u_0}{b} \tag{14}$$

where, u_0 represents the linear control law.

$$u_0 = \sum_{i=1}^{n} k_i(v_i - z_i) \tag{15}$$

At present, most industrial controls use PID controllers. LADRC can be obtained through the parameters of PID controller. The parameters obtained in this way can ensure that the system can realize a smooth transition from PID controller to LADRC system. In addition, nadrc parameters are difficult to adjust. Once the control parameters are improperly selected, it is very likely to lead to the unsatisfactory control effect of the system. LADRC can adjust parameters online based on bandwidth. According to the parameters of the existing PID controller, the initial value of LADRC can be selected, and then fine-tuning can achieve good control effect.

The conversion process from PID controller parameters to LADRC system control parameters is as follows.

The parameter expression of the known PID controller is as follows.

$$K_P(1 + \frac{1}{T_I S} + T_D S) = K_P + \frac{K_I}{S} + K_D S \tag{16}$$

$$K_I = \frac{K_P}{T_I}, K_D = K_P T_D \tag{17}$$

Suppose that the adjustable parameters K and L can be controlled by the controller bandwidth ω_c and observer bandwidth ω_0.

$$L = [\beta_1, \beta_2, \beta_3]^T, \beta_1 = 3\omega_0, \beta_2 = 3\omega_0^2, \beta_3 = \omega_0^3 \tag{18}$$

$$K = [K_1, K_2, 1]/b, K_1 = \omega_c^2, K_2 = 2\xi\omega_c^2 \tag{19}$$

First select α. α satisfy the following equation.

$$\omega_0^5 - \alpha K_d \omega_0^2 + 3\alpha K_P \omega_0 - 6\alpha K_i = 0 \tag{20}$$

The equation has at least five solutions, and there is at least one real solution. Hypothesis α If the value of is large enough, the equation can have a positive real solution. After the positive real solution is obtained, it can be set as the observer bandwidth.

In the second step, the bandwidth of the controller can be obtained through the following equation expression.

$$\begin{aligned} \omega_c &= \sqrt{\frac{\alpha K_i}{\beta_3}} \\ \xi &= \frac{\alpha K_p - \alpha K_i \beta_2/\beta_3}{2\omega_c \beta_3} \end{aligned} \tag{21}$$

Third, after obtaining the solution of β_1, β_2 and β_3, the gain b_0 can be obtained by the following equation expression.

$$b_0 = \frac{\alpha}{\beta_2 + K_P + \beta_1 K_d} \tag{22}$$

Through the above three steps, the parameters of LADRC and two bandwidth values can be obtained.

2.4 Comparative Simulation and Analysis

This paper simulates the linear active disturbance rejection control system. Suppose a controlled object is G_s.

$$G_s = \frac{1}{s^2 + 2s + 1} \tag{23}$$

PID parameters are adjusted through experience. The parameters of the three links are $k_p = 0.83$, $k_i = 0.33$, $k_d = 0.5$. Next, select $\alpha = 10000$. Therefore, the parameters of LADRC controller can be obtained according to the expression provided in the previous section as follows.

$$\omega_c = 0.98, \omega_0 = 15.09, b_0 = 12.74, \xi = 1.13 \tag{24}$$

This paper designs a comparative simulation experiment of PID system and LADRC system, as shown in Fig. 3.

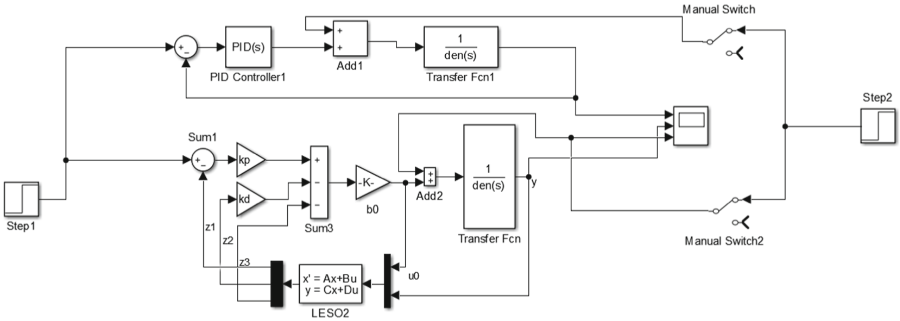

Fig. 3. Simulation diagram of PID and LADRC comparison

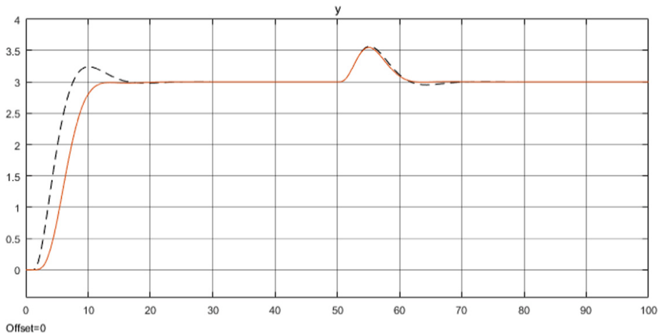

Fig. 4. Simulation result

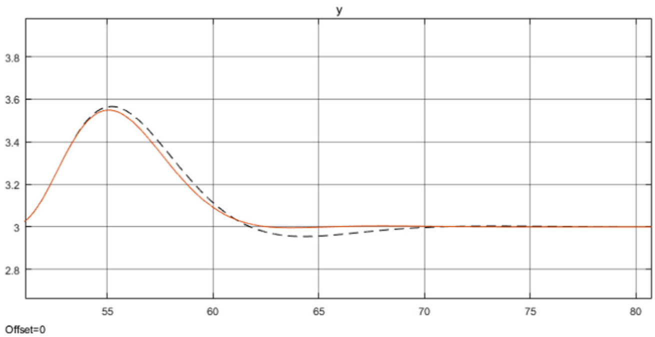

Fig. 5. Comparison curve of anti disturbance ability of two control systems in disturbance stage

Step2 module in Fig. 3 is a step response module. When the system runs to 50 s, the module will give the system a step response with a value of 1. The simulation results are as follows.

In Fig. 4, the black dotted line represents the response curve of PID. The red solid line represents the response curve of LADRC (Fig. 5).

According to the simulation results, it can be found that the anti-interference of LADRC. When the system is disturbed, the decline rate of the response curve of LADRC is greater than that of PID. At the same time, LADRC reduces the overshoot of the system in the low-frequency stage.

3 Research on ADRC System of Four Rotor UAV

3.1 Design of Attitude Control Module

Based on LADRC system, the attitude angle control sub module of inner loop control is improved again in this paper. The expression of UAV attitude angle control loop is as follows.

$$\begin{aligned} \ddot{\phi} &= f_2(\phi, \dot{\phi}, \dot{\theta}, \dot{\psi}, \omega, t, W_1, W_2, W_3, W_4) + b_2 U_2 \\ \ddot{\theta} &= f_3(\theta, \dot{\theta}, \dot{\phi}, \dot{\psi}, \omega, t, W_1, W_2, W_3, W_4) + b_3 U_3 \\ \ddot{\psi} &= f_4(\psi, \dot{\phi}, \dot{\theta}, \dot{\psi}, \omega, t, W_1, W_2, W_3, W_4) + b_4 U_4 \end{aligned} \tag{25}$$

$$\begin{bmatrix} b_2 \\ b_3 \\ b_4 \end{bmatrix} = \begin{bmatrix} 1/I_X \\ 1/I_Y \\ 1/I_Z \end{bmatrix} \tag{26}$$

where $f_1(\bullet)$, $f_2(\bullet)$ and $f_3(\bullet)$ are the total disturbances of the three angle channels of the UAV system respectively. The equation expression of height channel (Z channel) is as follows.

$$\ddot{z}_d = f_4(z, \dot{z}_d, t, W_1, W_2, W_3, W_4) + b_1 U_1/m - g \tag{27}$$

After obtaining the new attitude control loop designed based on LADRC controller, taking one of the rolling angle channels as an example, the LADRC controller is designed.

Rewrite the equation of the roll angle channel in expression (4.1) into the following state space equation form.

$$\begin{cases} \dot{x}_1 = x_2 \\ \dot{x}_2 = f_2(\phi, \dot{\phi}, \dot{\theta}, \dot{\psi}, \omega, t, W_1, W_2, W_3, W_4) + b_2 U_2 \\ y = x_1 \end{cases} \tag{28}$$

where, $f_2(\bullet)$ still represents the total disturbance of the system. So define $x_3 = f_2(\bullet)$, and $\dot{x}_3 = a(t)$. From the above expression, we can get the linear system after the expansion of expression (29).

$$\begin{cases} \dot{x}_1 = x_2 \\ \dot{x}_2 = x_3 + b_2 U_2 \\ \dot{x}_3 = a(t) \\ y = x_1 \end{cases} \tag{29}$$

So as to establish a new leso.

$$\begin{cases} e_l = z_1 - y \\ \dot{z}_1 = z_2 - \beta_1(e_l) \\ \dot{z}_2 = z_3 - \beta_2 e_l + b_2 u \\ \dot{z}_3 = -\beta_3 e_l \end{cases} \tag{30}$$

Let $z_1(t)$, $z_2(t)$ and $z_3(t)$ satisfy the following expressions.

$$\begin{aligned} z_1(t) &\to x_1(t) \\ z_2(t) &\to x_2(t) \\ z_3(t) &\to x_3(t) \end{aligned} \tag{31}$$

The expression of the control quantity U_2 is as follows.

$$U_2 = u_0 - z_3/b \tag{32}$$

The linear system expression can be obtained as follows.

$$\begin{cases} \dot{x}_1 = x_2 \\ \dot{x}_2 = bu_0 \\ y = x_1 \end{cases} \tag{33}$$

where, $u_0 = k_p(v_c - z_1) - k_d z_2$.

After calculating the attitude angle control equation and height control equation, a new attitude angle control module based on LADRC controller can be designed (Fig. 6).

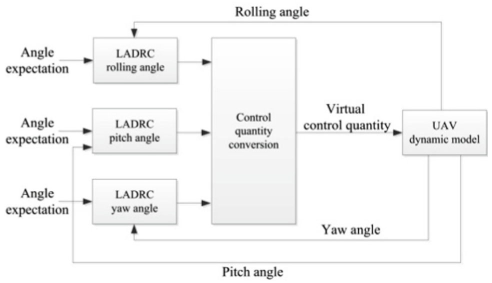

Fig. 6. Attitude angle control module

3.2 Simulation Results and Analysis

This paper uses four control parameters of PID to adjust the parameters of LADRC. The four control parameters are roll angle, pitch angle, yaw angle and Z-channel height. On this basis, the system is simulated. The simulation results are shown in the Figs. 7, 8, 9 and 10 below.

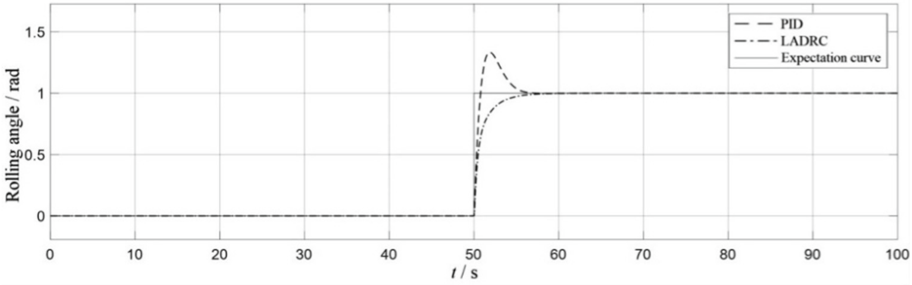

Fig. 7. Roll angle response curve

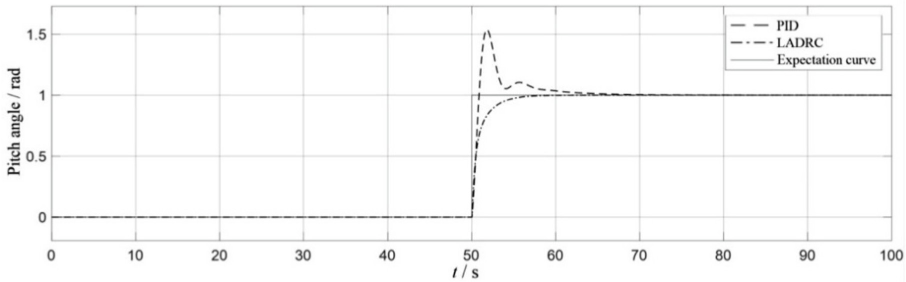

Fig. 8. Pitch angle response curve

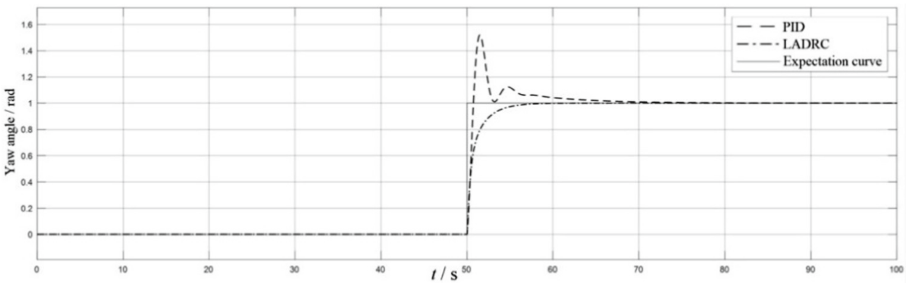

Fig. 9. Yaw angle response curve

At the moment of 50 s, sudden change interference is added to the angle control parameters. From the response curves of roll angle and pitch angle, it can be seen that the PID control system has a large overshoot, while the LADRC system changes smoothly. It can be seen that the small four rotor UAV system is an underactuated and strongly coupled system, and the disturbance inside the system can not be ignored. When using PID control system, PID is easy to cause imbalance in the face of system internal disturbance, and even cause instability of UAV flight control system. When LADRC system is used, overshoot caused by the system can be effectively suppressed.

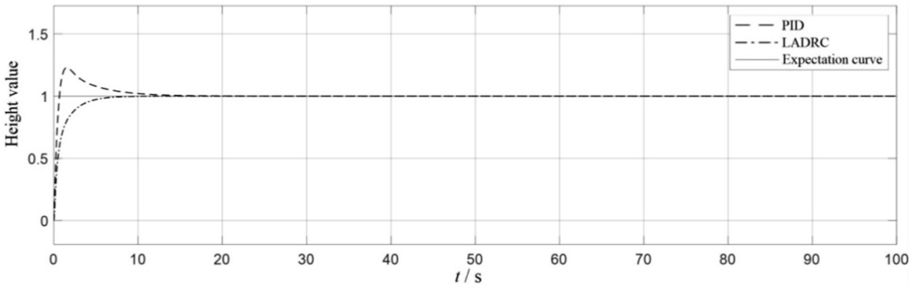

Fig. 10. z-channel response curve

4 Conclusion

This paper studies the effect of active disturbance rejection control method on the flight attitude of four rotor UAV. Firstly, the nonlinear active disturbance rejection algorithm is analyzed. Then a linear ADRC system model is designed. LADRC system and traditional PID control system are used to simulate the running state of the control object, and the differences between them are compared synchronously. The advantages and characteristics of LADRC system are verified. Finally, a LADRC scheme which can be used for flight attitude control of four rotor UAV is designed. The stability and effectiveness of the scheme are verified by simulation experiments. The research results have guiding significance for the flight control technology of multi rotor UAV.

Acknowledgment. This work was financially supported by the science and technology project of State Grid Hunan Electric Power Company Limited (5216A521001J).

References

1. Deng, C., Wang, S., Huang, Z., et al.: Unmanned aerial vehicles for power line inspection: a cooperative way in platforms and communications. J. Commun. **9**(09), 687–692 (2014)
2. Park, J., Kim, S., Lee, J., et al.: Method of operating a GIS-based autopilot drone to inspect ultrahigh voltage power lines and its field tests. J. Field Robot. **37**(03), 345–361 (2020)
3. Liu, C., Liu, Y., Wu, H., et al.: A safe flight approach of the UAV in the electrical line inspection. Int. J. Emerg. Electr. Power Syst. **16**(05), 503–515 (2015)
4. Shah, P., Agashe, S.: Review of fractional PID controller. Mechatronics **38**(01), 29–41 (2016)
5. Han, J.: From PID to active disturbance rejection control. IEEE Trans. Industr. Electron. **56**(03), 900–906 (2009)